Estuaries Vol. 12, No. 2, p. 66–81 June 1989

Abundance of Larval Rainbow Smelt (*Osmerus mordax*) in Relation to the Maximum Turbidity Zone and Associated Macroplanktonic Fauna of the Middle St. Lawrence Estuary[1]

JULIAN J. DODSON
JEAN-CLAUDE DAUVIN[2]
Département de biologie
Faculté des Sciences et de Génie
Université Laval
Sainte-Foy, Québec, G1K 7P4

R. GRANT INGRAM
B. D'ANGLEJAN
Institute of Oceanography
McGill University
3620 University St.
Montreal, Québec, H3A 2B2

ABSTRACT: We tested the hypothesis that the distribution and retention of larval smelt (*Osmerus mordax*) in the middle estuary of the St. Lawrence River is related to the maintenance of other planktonic organisms in the maximum turbidity zone (MTZ). We documented the horizontal and vertical distribution of larval smelt, macrozooplankton, and suspended particulate matter over four tidal cycles at each of three stations located along the major axis of the turbid upstream portion of the middle estuary. During summer, the turbid, warm, and low salinity waters of the two upstream stations were characterized by *Neomysis americana*, *Gammarus* sp. (principally *G. tigrinus*), larval smelt, *Mysis stenolepis*, and *Crangon septemspinosus*. The more stratified and less turbid waters of the downstream station were characterized by a coastal marine macrozooplanktonic community and the almost total absence of smelt larvae. Within the MTZ, the distribution of *N. americana* coincided with the zone of longest average advective replacement times (null zone). Smelt larvae were distributed further upstream within the MTZ than *N. americana*. Overall, larger larvae were distributed further upstream than smaller larvae. The relationship between turbidity and larval density at a specific time was weak (due to resuspension of sediments but not larvae), but the mechanism responsible for producing higher residence times for both sediment and larvae on a longer term basis appears the same. The daily movement and skewed nature of the null zone (due to the general cyclonic circulation of the middle estuary) defines a geographic zone over which the larval smelt population oscillates and remains despite the mean downstream velocities over the water column.

Introduction

The adaptive significance of retention of pelagic fish larvae in estuaries despite the net outflow of water is believed to be associated with the occurrence of optimal predator and prey conditions that favour larval survival (Leggett 1985). The fertilizing effect of nutrients derived from freshwater, offshore waters, and salt marshes, and their entrapment and rapid recycling within the estuary may all contribute to the high level of production characteristic of estuaries (Nixon 1981). Selective use of circulation to achieve landward penetration and retention in highly productive waters is now documented for a variety of aquatic organisms (reviewed by Leggett 1984; Miller et al. 1985). Although the benefits to larval fish of estuarine retention may be intuitively obvious, few studies have related the distribution of larval fish within the estuary to the trophic dynamics of estuaries.

An important sedimentological characteristic of many estuaries is the "maximum turbidity" or "en-

[1] Contribution to the program of GIROQ (Groupe Interuniversitaire de Recherche Océanographiques du Québec).

[2] Present address: Station Biologique, C.N.R.S. LP 4601 et Univ. P. et M. Curie (Paris VI), 29211 Roscoff, France.

0160-8347/89/020066-16$01.50/0

trapment" zone in which the concentration of suspended material is higher than in areas both landward and seaward. Such a turbidity maximum is a prominent feature of the upper portion of the middle St. Lawrence estuary (d'Anglejan and Smith 1973). The maximum turbidity zone (MTZ) extends from the Cap Tourmente tidal marsh on the north shore to downstream of Ouelle R. on the south shore in early spring; it retreats upstream during the summer months (Lucotte and d'Anglejan 1986). The MTZ starts and ends farther upstream in the north channel than in the south channel due to the general cyclonic circulation in the estuary (Kranck 1979).

The hydrodynamic forces responsible for maintaining maximum turbidity zones are similar to those involved in the landward transport and retention of pelagic organisms. Seaward-moving suspended matter settles from the surface layer to the landward-moving deep layer where it is carried back toward the head of the estuary and subsequently remixed into the surface layer. The repetition of this cycle builds up the concentration of suspended matter near the head of the estuary (Postma 1967; d'Anglejan and Ingram 1984). Other mechanisms involved in maintaining the St. Lawrence MTZ include flocculation during early salt mixing (Gobeil et al. 1981) and suspended sediment exchanges between the estuary and adjacent salt marshes (Lucotte and d'Anglejan 1986).

Maximum turbidity zones appear to be regions of high plankton density, due, presumably, to the common hydrodynamic control of suspended sediment and some pelagic components of the estuarine ecosystem. In the entrapment zone of the San Francisco Bay estuary, the concentration of nutritionally important compounds and the nutritional quality of the particulate matter is greater than in areas landward and seaward of the entrapment zone (Barclay and Knight 1981). These authors also observed that calanoid copepod nauplii and rotifers occurred at high concentrations in the entrapment zone and concluded that this zone is a nutritionally enhanced area for filter feeders. In the same estuary, the distribution and abundance of the estuarine opossum shrimp, *Neomysis mercedis,* a major part of the diet of a number of estuarine fish species, is related to the location of the entrapment zone (Siegfried et al. 1979). In the middle St. Lawrence estuary, Cardinal and Bérard-Therriault (1976) showed that the greatest concentrations of phytoplankton occurred at the upstream end of the MTZ in the area of Ile d'Orléans. In the same estuary, Bousfield et al. (1975) calculated that maximum zooplankton biomass is attained in the upper turbid freshwater and low-brackish region largely in the form of immature estuarine opossum shrimp (*Neomysis americana*), but to a significant extent by all stages of *Eurytemora affinis* and *Ectinosoma curticorne. N. americana* is the most common shallow-water mysid found in the western North Atlantic where it feeds on detritus, phytoplankton and crustaceans (Wigley and Burns 1971; Mauchline 1980). It has long been recognized as an important prey item for adult and juvenile fish in estuaries and may be an important trophic link between salt-marsh macrophyte production and higher trophic levels (Zagursky and Feller 1985). However, Bousfield et al. (1975) concluded that despite the apparently high secondary production of the region, the turbid upper estuary represents a "graveyard" for zooplankton entrapped there by their swimming behavior and the circulation, with no apparent link to the regional food pyramid.

Anadromous rainbow smelt (*Osmerus mordax*) larvae, one of the principal components of the ichthyoplankton community of the St. Lawrence estuary, are most abundant in the section of the middle estuary upstream of Ile aux Coudres (Fig. 1), where they are associated with warm and low salinity water masses (Able 1978; Courtois et al. 1982). Following the spring spawning season of smelt in the small rivers located along the south shore of the middle estuary, larval smelt disperse throughout the middle estuary where their distribution appears similar to that of suspended particulate matter (Ouellet and Dodson 1985). This observation led us to hypothesize that the distribution of smelt larvae in this area may be related to the retention of other planktonic organisms in the maximum turbidity zone, such that larvae would be concentrated in a region rich in potential food resources and thus form a link between the high secondary productivity of the turbid upper estuary and the estuarine food chain. As a first step in testing this hypothesis, we documented in 1985 the horizontal and vertical distribution of macrozooplankton, smelt larvae, and suspended sediment over four tidal cycles in relation to the MTZ at each of three stations situated in the upstream portion of the middle St. Lawrence estuary. As high densities of suspended matter and detritus rapidly clogged plankton net mesh sizes smaller than 0.5 mm, the densities of copepods and microzooplankton were not evaluated. In addition, we calculated the longitudinal and cross-channel flux of smelt larvae sampled within the MTZ to evaluate the degree of retention in this area.

Materials and Methods

Sampling Stations and Procedures

Three sampling stations (1, 2, 3; Fig. 1) were selected along an upstream-downstream transect

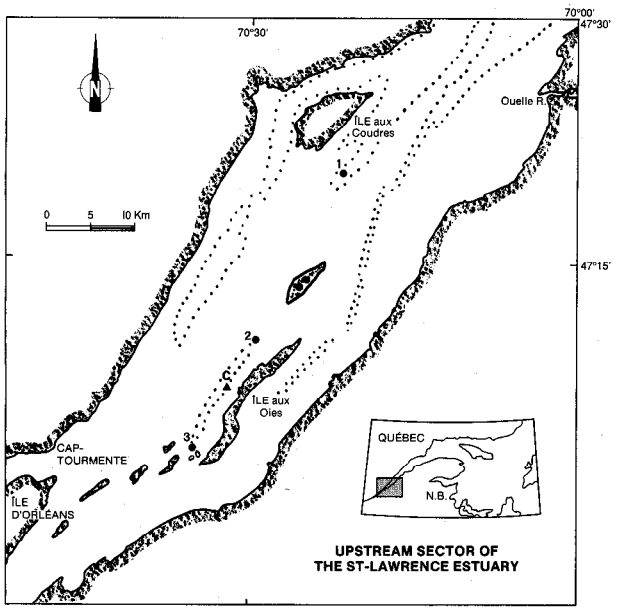

Fig. 1. Study area and location of current meter mooring (C) and sampling stations. Dotted lines illustrate the 20 m isobath.

located in the middle channel between Ile d'Orléans and Ile aux Coudres and sampled in their numerical order between July 23 and 30, 1985. Station 1 (mean depth: 20 m) was located at the approximate downstream end of the MTZ, near where a strong negative gradient in turbidity exists in the seaward direction. Stations 2 and 3 (mean depths: 18 m) were located 20 and 32 km upstream of station 1, respectively. Sampling was done with a 1-m² Tucker trawl fitted with an opening-closing device and a 0.5-m standard plankton net (0.500 mm mesh). A General Oceanic flowmeter fitted at the mouth of the net measured filtration rate. Towing speed varied from two to three knots. At each station, three discrete depth intervals were sampled hourly: a deep step-oblique tow from near the bottom to a depth of 12 m (bottom layer), a step-oblique tow from 12 to 6 m (middle layer) and a step-oblique tow from 6 m to the surface (surface layer). Each tow lasted 10 min.

The sampling program consisted of a 48-h series at each sampling station where the surface, middle, and bottom layers were successively sampled. Simultaneously with the plankton net tows, temperature, conductivity, and current velocity profiles were taken using an Aanderaa current meter in 1-m increments from a second boat anchored on station. Mean current speed for each depth layer was calculated by vector-averaging all of the profile values available. Turbidity (NTU) was measured simultaneously in water samples obtained with Niskin bottles at mid-depth in each depth stratum using a Hach Turbidity Meter. Concentrations of suspended matter (mg l^{-1}) by gravimetric filtration and particle size spectra by Coulter counter were determined near each high and low slack tide in the surface and bottom layers. The sequence of three 10-min plankton tows and profiling of physical variables was repeated hourly. Due to bad weather, sampling at station 1 was limited to 22 h July 23–24. Station 2 was sampled for 48 h July 26–28 and station 3 for 49 h July 28–30.

To further characterize the tidal current regime along the transect, a tide gauge and two Aanderaa current meters were moored at station C located 5 km upstream of station 2 between the 23 and 30 July (Fig. 1). Current meters were positioned 3 m and 12 m above the bottom.

Sample Treatment and Analysis

All biological samples were preserved in buffered 4% formalin. Plankton samples were completely sorted and organisms identified to calculate the density of smelt larvae and zooplankton. A maximum of 100 smelt larvae were randomly chosen from each sample, measured to the nearest 0.1 mm, and the mean length of larvae calculated for each sample. The density of smelt larvae was subsequently calculated for three size classes: L1 larvae <25 mm, L2 larvae 25–30 mm, and L3 larvae >30 mm. In the case of *Neomysis americana* and *Gammarus* sp., numbers were estimated volumetrically in samples containing more than 200 organisms. Densities of organisms were standardized for a 100 m³ volume of filtered water.

To describe the temporal structure of the macroplanktonic communities at stations 2 and 3 relative to the physical characteristics of the water masses, multivariate statistical analyses were carried out using seven biological variables to describe each sample—the densities of the decapod *Crangon septemspinosus*, the mysids *Neomysis americana* and *Mysis stenolepis*, the amphipods pooled as *Gammarus* sp. and the densities of each length class of smelt larvae. These variables were used to construct a chi² similarity matrix (Legendre and Legendre 1984) for each station. Using this measure of association, differences between the most abundant species contribute more to the similarity between samples than do differences between the rarer species. The hierarchical agglomerative clustering model of Lance and Williams (1967; flexible grouping with $\beta = -0.5$) was carried out to group the data from each station into homogenous clusters. The clustering of the samples was then superimposed on their projection in the reduced plane of the first two principal coordinates to separate the groups with the same planktonic composition. The principal axes were correlated (Kendall correla-

tions) with the biological variables in order to identify those variables contributing most to the separation of the groups. Finally, a multivariate discriminant analysis (Legendre and Legendre 1984) was applied to separate the groups on the basis of the physical variables, including temperature (°C), salinity (g kg^{-1}), and current speed (cm s^{-1}). The average values of these variables, coincident with each biological sample, were calculated for each depth stratum. In addition, turbidity (NTU) and the density of detritus present in the plankton net samples (ml per 100 m^3 of water filtered by net) were added to the matrix of physical data. Turbidity measured as NTU was significantly correlated with the concentration of suspended particulate matter ($Y(mg\ l^{-1}) = 1.347X(NTU) + 7.858$, $r = 0.84$, $n = 28$).

The flux of larvae at stations 2 and 3 was determined for each size class by multiplying the larval density in each depth interval by the mean velocity in that depth interval at the time of the net tows. Depth-integrated flux values were calculated as positive downstream and toward the north shore of the river. The actual depth of the bottom layer, using tidal height data, was employed in calculating depth-integrated values. To compare the magnitude and direction of flux among size classes and stations, flux is expressed as the number of larvae per meter of channel width per second.

Results

Physical Characteristics of the Sampling Area

This region of the St. Lawrence estuary can be characterized as a salt wedge type (Hansen and Rattray 1966). Mean tidal range at station C was 5 m over the 8-d sampling period. Stratification decreased in an upstream direction from station 1 to station 3. At station 3, surface salinities during the ebb were usually near zero with essentially no vertical stratification in the water column (Fig. 2). During the flood, maximum salinity differences were less than 0.8 g kg^{-1} between the surface and bottom layers. The mean gradient between the layers was 0.3 g kg^{-1}. At station 2, surface layer salinities ranged up to 2 g kg^{-1} during the flood and below 1 g kg^{-1} during the ebb (Fig. 2). Maximum salinity differences occurred during the flood when gradients reached 4 to 5 g kg^{-1} between the surface and bottom layers. Mean gradient between the layers was 1.4 g kg^{-1} during our anchor station. At station 1, surface layer salinities ranged from less than 7 to over 22 g kg^{-1} while the difference between the surface and bottom layers ranged from less than 2 g kg^{-1} during the ebb to over 6 g kg^{-1} during the flood. The mean gradient between the surface and bottom layers was 4 g kg^{-1}. Increasing salinity and decreasing temperature values with downstream distance were accompanied by increasing water column stratification on average. Because of the shallow depths in the study area, the anchor and the mooring station data indicate an interval late in the ebb of near zero stratification. Although the small salinity values are at the lower limit of accuracy for the Aanderaa instrument, resolution of salinity gradients was consistent (water column stability and T-S plots) at individual stations.

Turbidity increased in an upstream direction, with stations 2 and 3 situated well within the maximum turbidity zone (Fig. 2). At station 1, vertical turbidity gradients were weak, with mean values in the bottom layer reaching a maximum of 10 NTU at low tide. At stations 2 and 3, surface layer turbidity values remained fairly constant at about 15 NTU over the tidal cycle. In the bottom layers, turbidity values increased dramatically over the tidal cycle being maximal (>100 NTU) during the flood (Fig. 2). At station 2, bottom layer turbidity values declined to 50 NTU at high tide and during the ensuing ebb tide and increased to 75 NTU at the end of ebb. At station 3, bottom turbidity values declined to less than 30 NTU at high tide and increased to 70 NTU during the ensuing ebb before decreasing to 50 NTU at the end of ebb (Fig. 2).

The size distribution of the suspended particle population followed a log-normal distribution, in agreement with the previous measurement of Kranck (1979). At station 1, the median size increased significantly between the surface and bottom layers, from around 6 μm to around 10 μm at low and high tides respectively. At stations 2 and 3, particle median size remained identical with time (between 6 and 8 μm) in both layers, in spite of considerably higher concentrations in the bottom layer.

Peterson et al. (1975) reported that the longest average advective replacement times, relative to areas situated further upstream or downstream, occur in the "null zone." Our moored and profiling current meter data indicate that the null zone was initially situated slightly upstream of station 2 during the study period. Mean bottom layer flow at station 1 was strongly upstream. At station C, a progressive vector diagram (calculated from the current meter record obtained at a height of 3 m above the bottom) showed a net downstream motion at the beginning of the mooring and near zero mean motion (calculated over a semidiurnal tidal cycle) over July 26–30. A strong cross-channel flow (SE) was noted at the lower moored instrument at the start of the ebb flow for each tide cycle. No

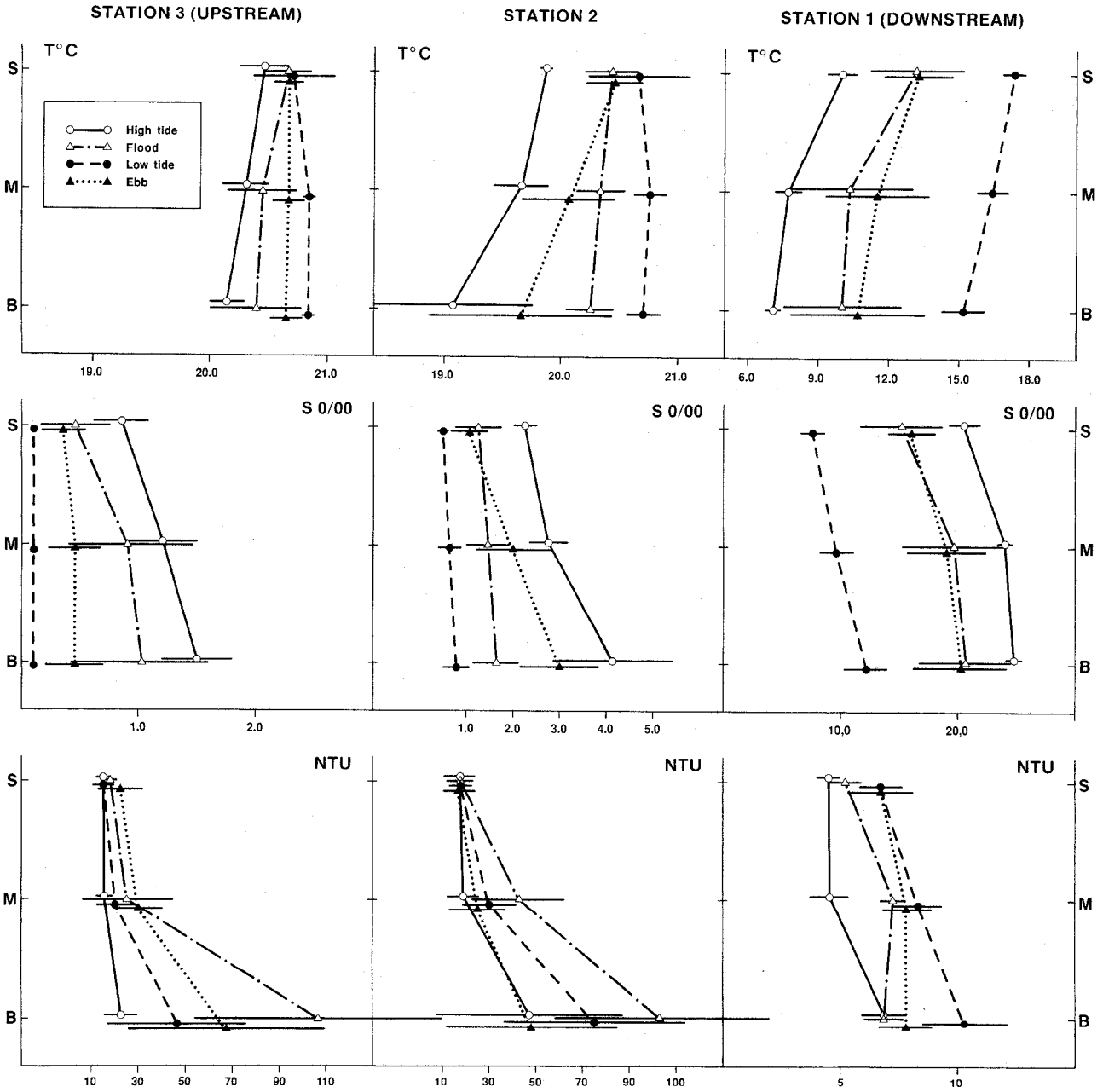

Fig. 2. Principal physical characteristics of the three stations sampled in July 1985. Mean values and standard deviations (horizontal lines) of temperature (°C), salinity (‰) and turbidity (NTU) measured at high tide (±1 h), low tide (±1 h), flooding tide and ebbing tide are presented for three depth layers: surface layer (S: 0–6 m), middle layer (M: 6–12 m), and bottom layer (B: 12–18 m). Note that scales for temperature, salinity, and turbidity are not the same for all stations.

similar feature was seen at the upper current meter. Averaged over the complete record, there was a net cross-channel drift to the south shore. This indicates that the null zone (in an along-channel sense) was in the vicinity of station C after July 26 and close to station 2 prior to July 26. The retreat of the null zone resulted from a decrease in amplitude of the low frequency (less than diurnal) flow. Record length was too short to separate runoff changes and meteorologically forced effects.

Spatial Organization of the Macroplanktonic Community

A spatial difference in species diversity was observed (Table 1), with 20 macroplanktonic species occurring at the downstream end of the transect

TABLE 1. Occurrence of macroplankton at three stations sampled at the upstream end of the middle St. Lawrence estuary in July 1985.

Taxon	Station 1	Station 2	Station 3
Mysidacea			
Mysis littoralis	+		
Mysis stenolepis	+	+	+
Neomysis americana	+	+	+
Isopoda			
Jaera albifrons	+	+	
Idothea phosphorea	+		
Amphipoda			
Atylus carinatus	+		
Calliopius laeviusculus	+	+	
Dyopedos monacanthus	+		
Gammarus laurencianus	+	+	
Gammarus oceanicus	+	+	
Gammarus setosus	+		
Gammarus tigrinus		+	+
Monoculodes edwardsi	+		
Phoxocephalus holbolli	+		
Weyprechtia heuglisci	+		
Euphausiacea			
Meganyctiphanes norvegica	+		
Thysanoessa inermis	+		
Thysanoessa longicaudata	+		
Decapoda			
Crangon septemspinosus	+	+	+
Chaetognatha			
Sagitta elegans	+		
Pisces			
Osmerus mordax	+	+	+
Microgadus tomcod		+	+
Morone americana			+

and 7 species at the upstream end. Oligohaline and mesohaline species such as *Neomysis americana* and *Crangon septemspinosus* occur throughout the region, whereas coastal marine species such as *Sagitta elegans* and the euphausids are restricted to station 1. The capture at night of several species of benthic amphipods also contributed to the greater species diversity of station 1. Ichthyoplankton species diversity was poor during the study period. Smelt larvae occurred throughout the region, young-of-the-year tomcod (*Microgadus tomcod*) were abundant at stations 2 and 3, and larval white perch (*Morone americana*) occurred rarely at station 3.

An examination of the densities of the dominant taxa of macroplankton reveals that *N. americana*, *Gammarus* sp., and smelt larvae are respectively 72, 62, and 23 times more abundant at the upstream end of the transect than at the downstream end (Table 2). The two upstream stations, situated within the maximum turbidity zone, are characterized by low salinities and high concentrations of suspended particulate matter. Within the MTZ, the densities of *N. americana*, *M. stenolepis*, and *C. septemspinosus* appear to decline from station 2 to station 3 whereas the densities of *Gammarus* sp. and smelt larvae increase. In addition, smelt larvae sampled at station 1 are smaller than those sampled within the MTZ (Table 2).

Temporal Structure of the Macroplanktonic Communities

Downstream Station

The temporal structure of the macroplanktonic community at the downstream end of the maximum turbidity zone (station 1) was clearly related to tidal state (Fig. 3). High temperature (14.1 °C, SD = 2.8) and low salinity (13.8 g kg^{-1}, SD = 4.5) water masses occurring at low tide and during the first part of the flood were characterized by relatively high densities of *N. americana* and small smelt larvae (Table 2, Fig. 3). Low temperature (8.4 °C, SD = 1.6) and high salinity (22.8 g kg^{-1}, SD = 2.5) water masses occurring at high tide were characterized by marine species such as euphausids and the almost total absence of smelt larvae.

TABLE 2. Abundance (N per 100 m^3) of the dominant macroplanktonic taxa and mean length (mm) of smelt larvae at three stations sampled at the upstream end of the middle St. Lawrence estuary in July 1985. $\bar{x}$ = mean, s = standard deviation, min = minimum value, max = maximum value.

	Station 1				Station 2				Station 3			
	$\bar{x}$	s	Min	Max	$\bar{x}$	s	Min	Max	$\bar{x}$	s	Min	Max
Gammarus sp.	1.8	3.6	0	10.4	77.8	106.6	0	625.6	111.4	161.0	0	1,536.0
Neomysis americana	27.9	72.3	0	392.1	2,328.9	2,527.1	2.3	15,057.4	1,714.5	3,130.6	0	16,296.0
Mysis stenolepis	2.4	4.7	0	24.9	16.7	27.2	0	196.3	3.3	6.5	0	38.9
Crangon septemspinosus	0.9	0.5	0	1.9	1.1	2.5	0	25.9	0.1	0.0	0	0.3
Euphausiacea	1.2	3.0	0	14.2	—	—	—	—	—	—	—	—
Total *Osmerus mordax*	1.8	3.6	0	15.2	26.1	27.3	0.3	187.3	41.9	54.1	1.9	531.6
O. m. L1	1.4	2.9	0	14.5	9.2	11.2	0	66.5	6.8	8.9	0	75.3
O. m. L2	0.3	0.9	0	5.5	9.3	13.1	0	97.4	22.1	30.7	0	284.6
O. m. L3	0.1	0.3	0	1.4	7.7	9.1	0	56.2	13.4	19.8	0	214.8
O. m. mean length	20.8	4.3	18.5	27.0	27.2	2.6	21.9	32.5	28.5	1.5	25.6	34.1

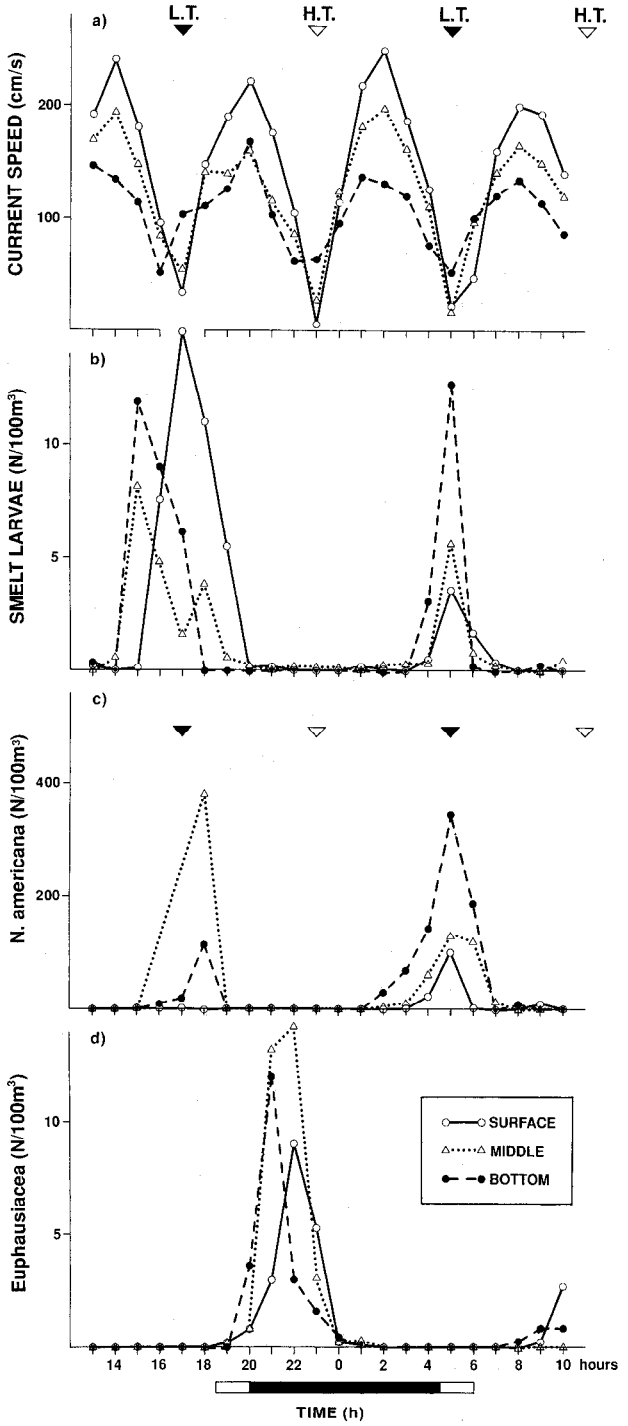

Fig. 3. The results of the 22-h sampling series (July 23–24) conducted at three depth layers at station 1. (a) tidal current speed, (b) abundance of smelt larvae, (c) abundance of *N. americana*, (d) abundance of Euphausiacea. L.T. = low tide, H.T. = high tide. Dark horizontal bar indicates night hours and open horizontal bars, dawn and dusk.

Median Station

The clustering of the 144 samples obtained at station 2 at a similarity level of 0.94 resulted in three groups (Fig. 4). Group 1 was composed of 17 samples obtained principally one or two hours before or after high tide. Group 2 was composed of 81 samples obtained from three hours before to three hours after low tide and group 3 was composed of 46 samples obtained at high tide.

Principal coordinate analysis revealed that 87.5% of the total variance was explained by the first two principal axes (axis 1 = 64.9%, axis 2 = 22.6%). The first axis, positively correlated with the density of the smallest length class of smelt larvae and of *C. septemspinosus* and negatively correlated with the densities of the intermediate and largest length classes of smelt larvae, *N. americana*, and *Gammarus* sp. (Table 3), contributes to separating the three groups (Fig. 5). The second axis, positively correlated with the densities of all length classes of smelt larvae and *N. americana* and negatively correlated with the densities of *Gammarus* sp. and *C. septemspinosus* (Table 3), illustrates the great dispersion of the samples of groups 1 and 3 relative to the concentration of the samples of group 2 in factorial space (Fig. 5).

The first function of the discriminant analysis carried out to separate the groups on the basis of the physical characteristics of the environment (Wilks' Lambda = 0.85, p = 0.015) explained 99.6% of the intergroup variance (Fig. 5) and was correlated mainly with temperature and salinity (Table 4). The second function was mainly correlated with tidal current speed (Table 4).

In summary, temporal variations in the biological characteristics of the median station were less pronounced than those observed at the downstream station. Group 2, associated with the lower salinity water masses occurring on the ebbing and low tide, is characterized by high densities of intermediate and large smelt larvae and high densities of *N. americana* (Table 5). Groups 1 and 3 are both associated with the lower temperature and higher salinity water masses occurring around high tide. Group 1 is characterized by high densities of small smelt larvae and relatively high densities of *C. septemspinosus*. Group 2 exhibits densities of smelt larvae, *N. americana*, and *C. septemspinosus* intermediate to those observed for groups 1 and 3.

The temporal evolution of the major characteristics at station 2 are illustrated in Fig. 6. Minimum densities of *N. americana* generally occur during flood, with maximum densities generally occurring during ebb. At station 2, larval mean lengths at all depths increased to maximum values at the end of ebb and decreased during the ensuing flood, al-

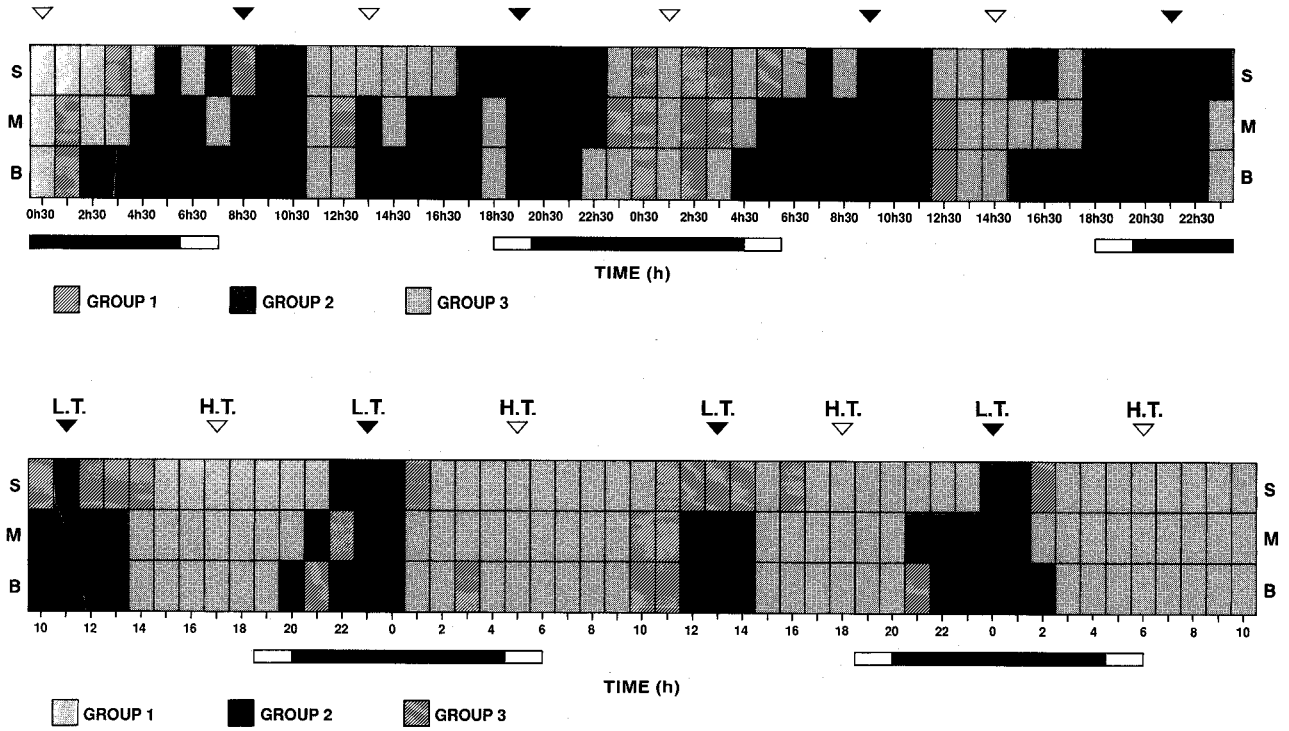

Fig. 4. Upper panel. Temporal presentation of the clustering of samples obtained at station 2, July 26–28, 1985, by the hierarchical agglomerative clustering model of Lance and Williams (1967; similarity level of 0.94). Lower panel. Temporal presentation of the clustering of samples obtained at station 3, July 28–30, 1985, by the hierarchical agglomerative clustering model of Lance and Williams (1967; similarity level of 0.94). S = surface layer, M = middle layer, B = bottom layer, L.T. = low tide, H.T. = high tide. Dark horizontal bars indicate night hours and open horizontal bars, dawn and dusk.

though the relationship begins to break down at the end of the series. Maximum densities of smelt larvae were observed prior to daytime low tides. This 24-h cycle in smelt abundance may be due to an asymmetry of ebbing tides observed at this station. Morning ebbs attained greater speeds and lasted 8 h, whereas evening ebbs were weaker and lasted 7 h. This observation coupled with the evo-

TABLE 3. Kendall correlation coefficients and probability levels (in parentheses) between the biological variables and the first two principal axes (C1, C2) of the principal coordinate analyses of two stations sampled in the middle estuary of the St. Lawrence River, July 1985. L1, L2, L3 denote three length classes of smelt larvae. n.s. = not significant.

Biological Variables	Station 2		Station 3	
	C1	C2	C1	C2
Osmerus mordax, L1	0.315 (<0.0001)	0.200 (0.0004)	0.231 (<0.0001)	0.285 (<0.0001)
Osmerus mordax, L2	−0.140 (0.013)	0.180 (0.0015)	0.356 (<0.0001)	0.126 (0.0241)
Osmerus mordax, L3	−0.319 (<0.0001)	0.149 (0.0083)	n.s.	0.183 (0.001)
Gammarus sp.	−0.172 (0.0024)	−0.541 (<0.0001)	0.226 (<0.001)	−0.563 (<0.0001)
Neomysis americana	−0.651 (<0.0001)	0.119 (0.0351)	−0.768 (<0.0001)	n.s.
Mysis stenolepis	n.s.	n.s.	−0.633 (0.0001)	n.s.
Crangon septemspinosus	0.243 (<0.0001)	−0.119 (0.0448)	−0.196 (0.0036)	n.s.

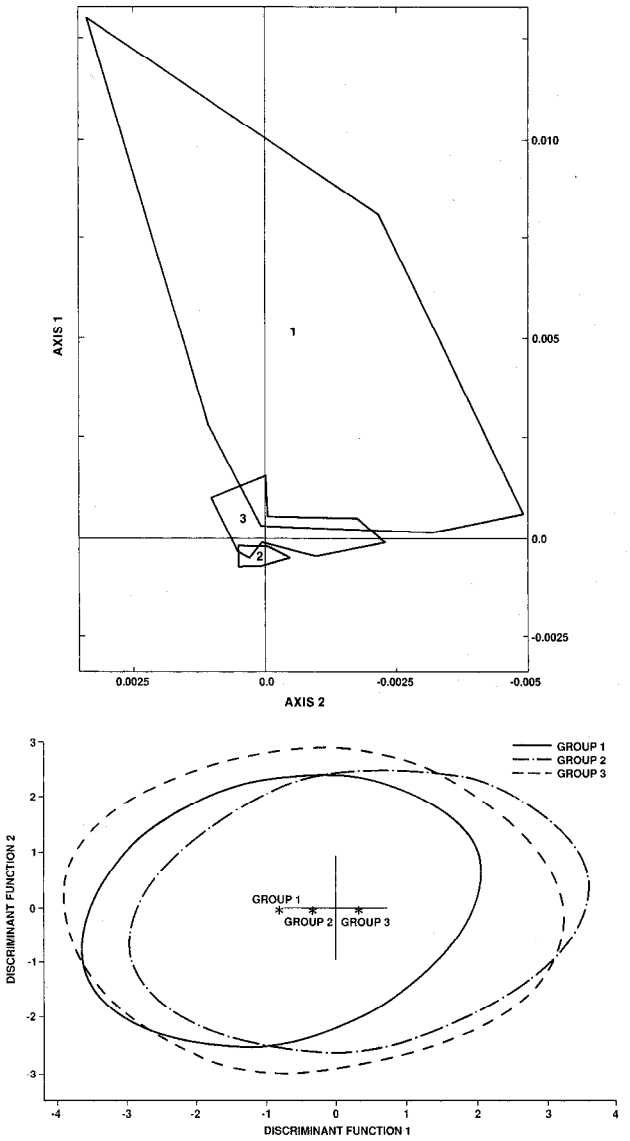

Fig. 5. Upper panel. Relation of station 2 sample groups to biological variables. The three clusters of samples are superimposed on their projection in the reduced plane of the first two principal axes. Lower panel. Relation of station 2 sample groups to physical variables. Position of centroids and ellipses englobing the three clusters of biological samples are plotted in the reduced plane of discriminant functions 1 and 2.

TABLE 5. Mean densities and standard deviations (in parentheses) of three length classes of smelt larvae and the macrozooplankton of the sample groups obtained at station 2, St. Lawrence middle estuary, July 1985. Densities expressed as number 100 m^{-3}.

Variable	Group 1	Group 2	Group 3
Osmerus mordax, L1	17.90 (15.01)	6.52 (7.13)	10.53 (13.53)
Osmerus mordax, L2	4.92 (4.88)	12.16 (15.54)	5.86 (8.31)
Osmerus mordax, L3	2.31 (2.07)	10.71 (10.24)	4.31 (5.81)
Gammarus sp.	85.78 (122.67)	83.33 (86.69)	65.03 (130.96)
Neomysis americana	175.94 (145.77)	3,513.87 (2,684.29)	1,037.97 (1,222.34)
Mysis stenolepis	12.78 (12.13)	11.05 (17.24)	27.99 (39.65)
Crangon septemspinosus	3.04 (5.97)	0.56 (1.22)	1.28 (1.32)

lution of larval mean length suggests the advection of high densities of large smelt larvae from upstream during strong ebbs.

At station 2, the largest flux contributions occurred at times of highest larval densities, early and late in the ebb flow. Small smelt larvae were mainly observed early in the ebb, whereas medium size and large larvae were predominately observed late in the ebb (Fig. 7). The time- and depth-integrated flux of small larvae over the 48-h study period was downstream (0.76 larvae m^{-1} s^{-1}) and toward the north shore (0.02 larvae m^{-1} s^{-1}). A similar relationship was found for medium size (0.76 larvae m^{-1} s^{-1} and 0.07 larvae m^{-1} s^{-1}, downstream and toward the north shore, respectively) and large smelt larvae (0.61 larvae m^{-1} s^{-1} and 0.06 larvae m^{-1} s^{-1}, downstream and toward the north shore, respectively).

Upstream Station

The clustering of the 147 samples obtained at station 3 at a similarity level of 0.8 resulted in three groups (Fig. 4). Group 1 was composed of 89 samples principally obtained three hours before and after high tide and group 2 composed of 39 samples

TABLE 4. Mean values and standard deviations (in parentheses) of the physical variables characterizing the groups of samples obtained at the station 2, middle St. Lawrence estuary, July 1985, and their contribution (standardized canonical coefficients) to the formation of two discriminant axes (1, 2). Numbers in parentheses indicate rank in decreasing order of importance. The percentage of samples of each group correctly classified in their group of origin is also indicated (% class).

Variable	Group 1	Group 2	Group 3	1	2
Salinity (g kg^{-1})	2.6 (1.6)	1.6 (1.4)	2.1 (1.0)	0.8 (2)	−0.1 (3)
Temperature (°C)	19.7 (0.8)	20.3 (0.6)	19.9 (0.5)	1.7 (1)	−0.0 (4)
Tidal speed (cm s^{-1})	66.7 (42.9)	72.2 (35.2)	71.5 (41.2)	−0.2 (4)	0.9 (1)
Turbidity (NTU)	28.0 (26.8)	37.3 (32.6)	31.6 (32.7)	−0.0 (5)	0.0 (5)
Detritus (ml 10 m^{-3})	13.8 (21.0)	37.6 (52.0)	24.0 (55.9)	0.5 (3)	−0.3 (2)
% class	41.2	79.0	56.5		

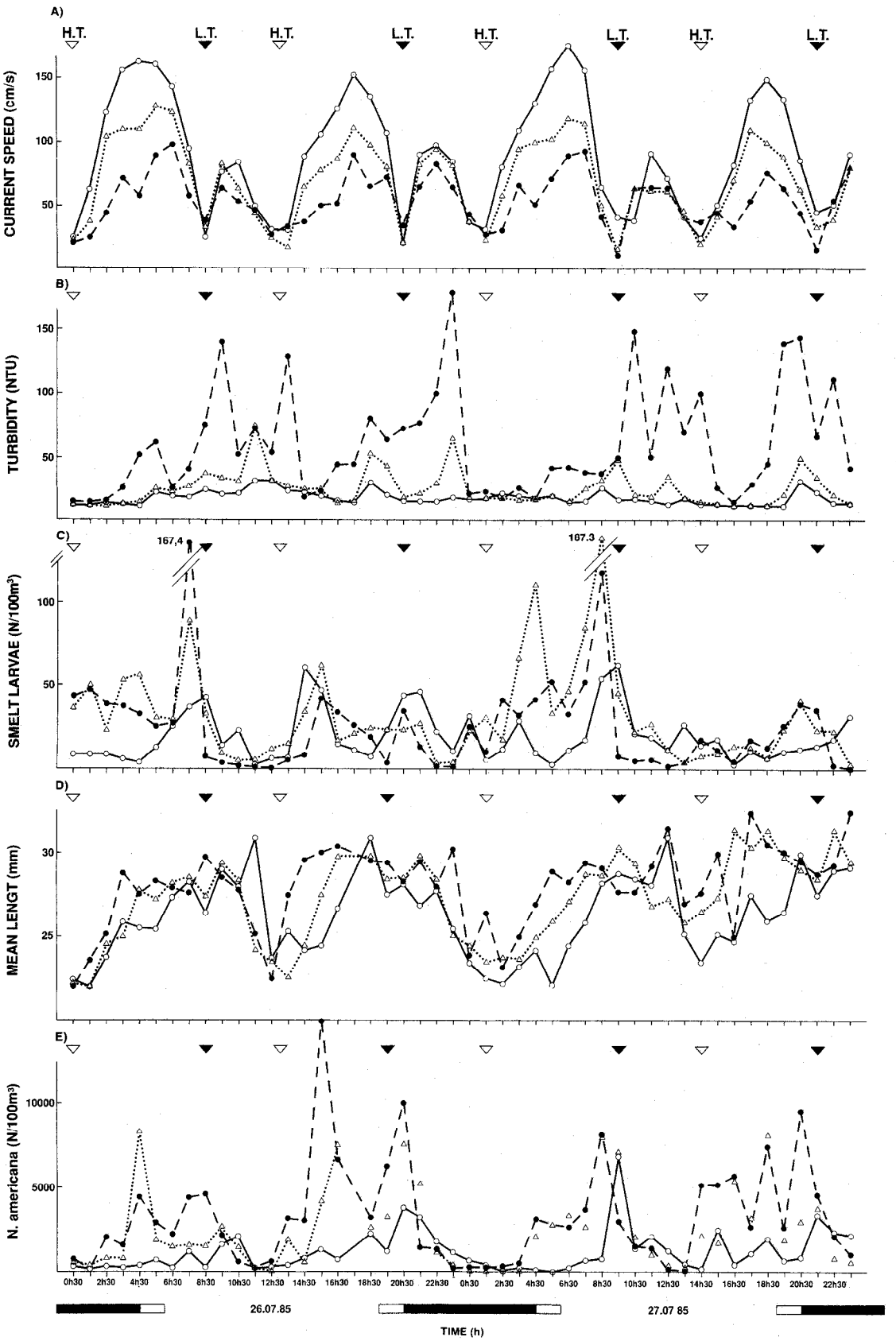

Fig. 6. The results of the 48-h sampling series (July 26–28) conducted at three depth layers at station 2. (A) tidal current speed, (B) turbidity (NTU), (C) abundance of smelt larvae, (D) mean length (mm) of smelt larvae, (E) abundance of *N. americana*. L.T. = low tide, H.T. = high tide. Dark horizontal bars indicate night hours and open horizontal bars, dawn and dusk.

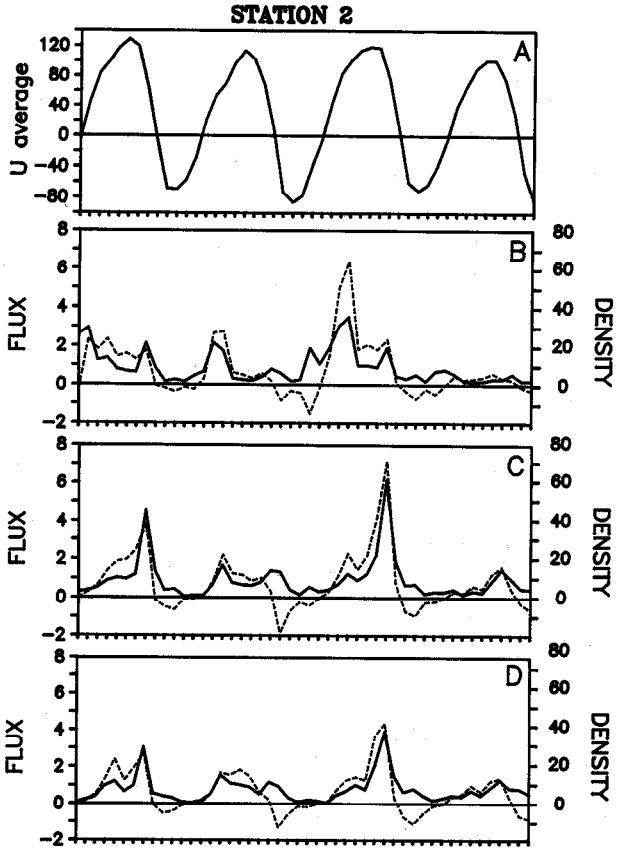

Fig. 7. Density and flux of smelt larvae at station 2. Panel A. Average depth-integrated longitudinal current velocity (cm s^{-1}) measured during the study period (positive values, downstream; negative values, upstream). The density (n 100 m^{-3}) and depth-integrated flux (n m^{-1} s^{-1}) of smelt larvae <25 mm, 25–30 mm, and >30 mm are presented in panels B, C, and D, respectively. The solid line illustrates larval density and the dotted line illustrates larval flux (positive values, downstream; negative values, upstream).

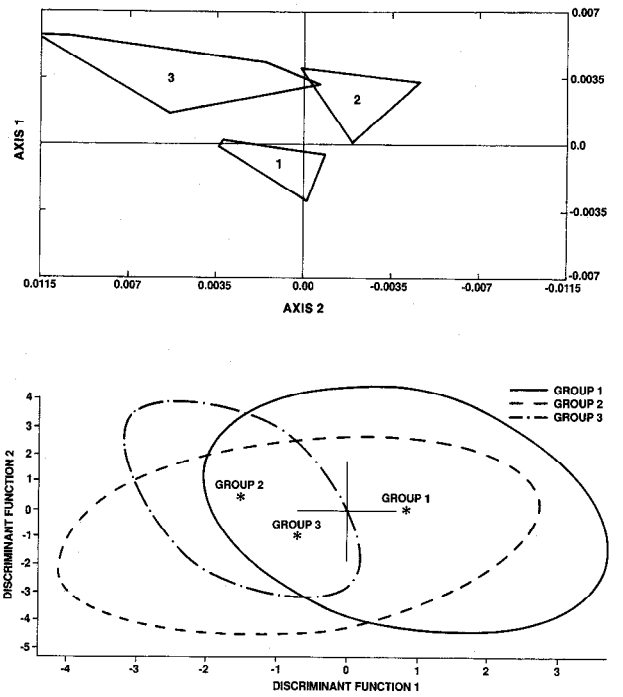

Fig. 8. Upper panel. Relation of station 3 sample groups to biological variables. The three clusters of samples are superimposed on their projection in the reduced plane of the first two principal axes. Lower panel. Relation of station 3 sample groups to physical variables. Position of centroids and ellipses englobing the three clusters of biological samples are plotted in the reduced plane of discriminant functions 1 and 2.

obtained at low tide. Group 3 is composed of 19 samples obtained during daytime low tides.

Principal coordinate analysis revealed that 93.8% of the total variance was explained by the first 2 principal axes (axis 1 = 58.0%, axis 2 = 35.8%). The first axis (Table 3), positively correlated with the densities of the small and intermediate size classes of smelt larvae and *Gammarus* sp. and negatively correlated with the densities of *N. americana, M. stenolepis,* and *C. septemspinosus,* separates groups 2 and 3 from group 1 (Fig. 8). The second axis, positively correlated with the densities of all classes of smelt larvae and negatively correlated with *Gammarus* sp., contributes to separating group 2 from group 3.

The first function of the discriminant analysis carried out to separate the groups on the basis of the physical characteristics of the environment (Wilks' Lambda = 0.42, $p < 0.0001$) explained 88% of the intergroup variance (Fig. 8) and was correlated mainly with salinity (Table 6). The second function was mainly correlated with current speed.

To summarize, group 1, associated with the more saline water masses occurring around high tide, is characterized by high densities of *N. americana* (Table 7). Groups 2 and 3 are associated with the lower salinity water masses occurring around low tide. Group 2 is characterized by high densities of *Gammarus* sp. and intermediate size smelt larvae. Group 3, the most poorly defined group in terms of physical characteristics (Table 6), is characterized by high densities of all size classes of smelt larvae.

The temporal evolution of the major characteristics of station 3 is illustrated in Fig. 9. Maximum densities of *N. americana* are associated with the flooding tide whereas maximum densities of *G. tigrinus,* the principal gammarid at this station, occur around low tide. Smelt larvae are most abundant at maximum values of both ebb and flood currents and coincide with maximum turbidity values in the bottom layer. Although no definite pattern can be seen in the variation of larval size, there is a tendency for the mean length of larvae sampled in the intermediate and bottom layers to increase prior

TABLE 6. Mean values and standard deviations (in parentheses) of the physical variables characterizing the three groups of samples obtained at station 3, middle St. Lawrence estuary, July 1985, and their contribution (standardized canonical coefficients) to the formation of two discriminant axes (1, 2). Numbers in parentheses indicate rank in decreasing order of importance. The percentage of samples of each group correctly classified in their group of origin is also indicated (% class).

Variable	Group 1	Group 2	Group 3	1	2
Salinity (g kg^{-1})	0.9 (0.53)	0.1 (0.1)	0.2 (0.3)	1.8 (1)	0.6 (2)
Temperature (°C)	20.4 (0.3)	20.8 (0.1)	20.7 (0.3)	0.4 (3)	0.5 (3)
Tidal speed (cm s^{-1})	71.2 (37.2)	63.2 (30.1)	97.9 (27.7)	0.5 (2)	−0.9 (1)
Turbidity (NTU)	33.2 (33.9)	36.9 (37.6)	23.8 (12.2)	−0.1 (5)	0.2 (5)
Detritus (ml 10 m^{-3})	12.5 (21.7)	20.2 (29.3)	8.7 (9.3)	−0.1 (4)	0.5 (4)
% class	82.0	94.9	31.6		

to high tide and subsequently decrease during ebb. These observations suggest that *N. americana* and larger smelt larvae are advected from downstream during floods, whereas *G. tigrinus* and smaller smelt larvae are advected from upstream during ebbs.

At station 3, the densities of small smelt larvae were high during both the flood and the ebb (Fig. 10). The time- and depth-integrated flux of small larvae over the 49-h study period was slightly upstream (−0.04 larvae m^{-1} s^{-1}). There was evidence of input of small larvae from the north at this site. The net flux of medium size larvae over the study period was slightly upstream (−0.07 larvae m^{-1} s^{-1}) and toward the north shore (0.03 larvae $m^{-1}s^{-1}$). Stronger floods were associated with increased larval densities and short-lived, high, upstream flux values. A similar relationship was found for large larvae, except that net flux over the study period was more strongly upstream (−0.23 larvae m^{-1} s^{-1}) and toward the south shore (−0.06 larvae m^{-1} s^{-1}).

Discussion

The spatial distribution of smelt larvae in the middle portion of the St. Lawrence estuary is clearly associated with the maximum turbidity zone. During summer, the turbid, warm, and low salinity waters of stations 2 and 3 were characterized by *N. americana, Gammarus* sp. (principally *G. tigrinus*), larval smelt, *Mysis stenolepis,* and *Crangon septemspinosus,* whereas the more stratified and less turbid waters of station 1 were characterized by a coastal marine macrozooplanktonic community. At station 1, the presence of low densities of *N. americana* and smelt larvae in association with warmer, less saline water masses at low tide indicates that this station was located at the downstream end of the maximum turbidity zone and its associated fauna during the study period.

Our observations complement those of Bousfield et al. (1975) who sampled the middle estuary along an upstream-downstream gradient using pumps. They identified three major groups of species: (1) freshwater species; the cladoceran *Bosmina longirostris* and *Daphnia* sp. characterized the turbid upstream waters where summer temperatures exceeded 19°C and salinities varied between 0 and 2 g kg^{-1}, conditions prevailing at our station 3; (2) estuarine endemic species; *Eurytemora affinis, E. herdmani, N. americana, M. stenolepis, M. gaspensis,* and *Ectinosoma curticorne* characterized turbid waters varying between 10° and 20°C and between 0 and 10 g kg^{-1}, conditions similar to those observed at our stations 2 and 3; and (3) marine coastal species; *Calanus finmarchicus, Acartia clausi,* and *A. longiremis* characterized the colder, more saline waters typical of our station 1. These authors also observed an upstream-downstream gradient in zooplankton density. Copepod densities in the vicinity of our station 3 were greater than 220,000 organisms per 100 m^3, between 130,000 and 220,000 organisms per 100 m^3 in the vicinity of station 2, and between 11,000 and 48,000 organisms per 100 m^3 near station 1. Densities of cladocera also declined from station 3 to station 2.

Average densities of macrozooplankton in the present study were less at the downstream end of the maximum turbidity zone as were maximum densities (Table 2). However, these densities are

TABLE 7. Mean densities and standard deviations (in parentheses) of three length classes of smelt larvae and the macrozooplankton of the three sample groups obtained at station 3, St. Lawrence middle estuary, July, 1985. Densities expressed as N. 100 m^{-3}.

Variable	Group 1	Group 2	Group 3
O. mordax, L1	6.11 (9.48)	4.66 (3.39)	14.32 (10.27)
O. mordax, L2	17.22 (33.77)	23.04 (16.12)	42.88 (30.69)
O. mordax, L3	15.49 (24.24)	7.25 (4.83)	16.51 (11.99)
Gammarus sp.	56.54 (64.73)	258.48 (239.50)	66.50 (69.60)
N. americana	2821.38 (3621.77)	19.68 (65.34)	8.04 (9.42)
M. stenolepis	5.39 (7.62)	0.00 (0.04)	0.18 (0.81)
C. septemspinosus	0.02 (0.07)	0.00 (0.00)	0.00 (0.00)

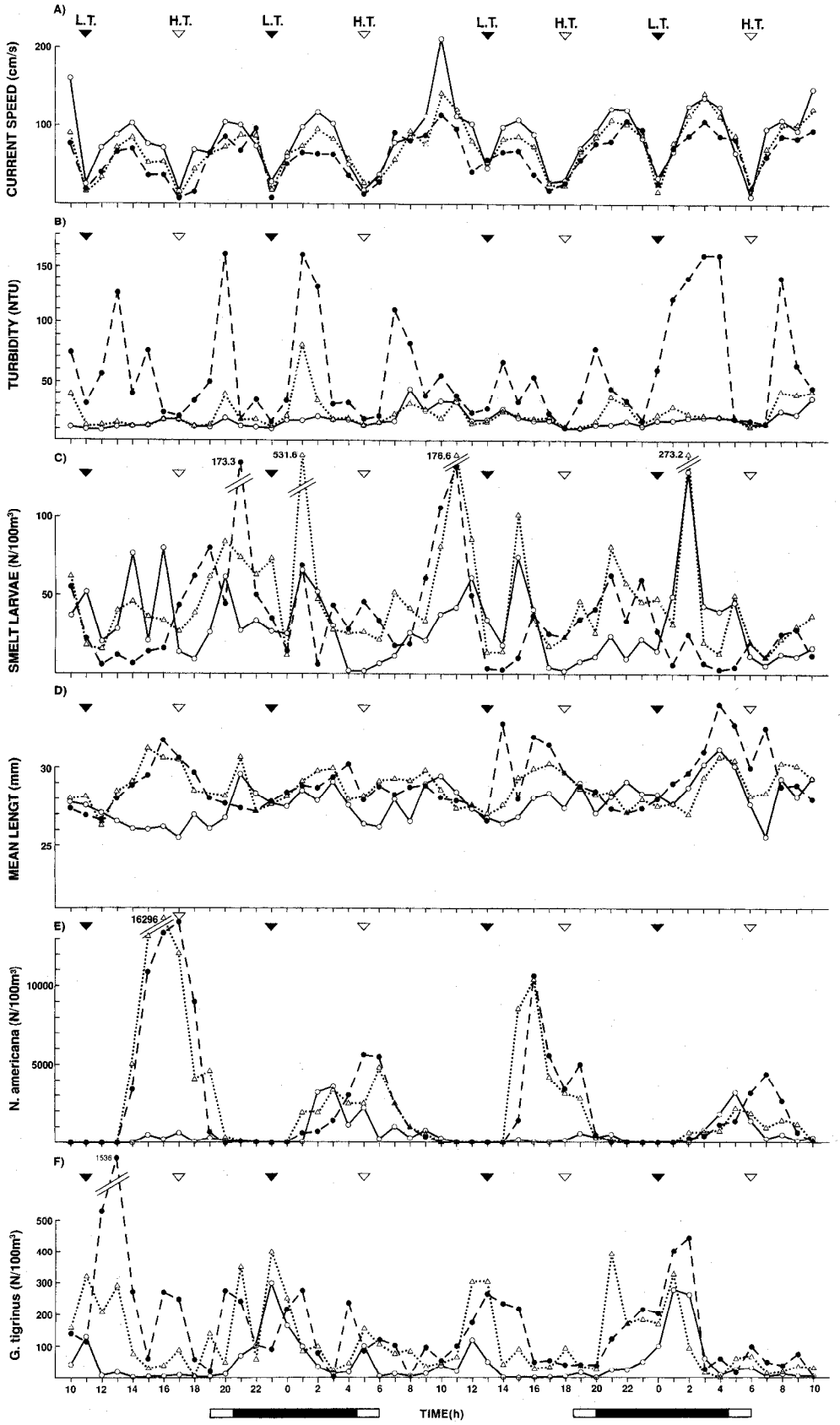

Fig. 9. The result of the 49-h sampling series (July 28–30) conducted at three depth layers at station 3. (A) tidal current speed, (B) turbidity (NTU), (C) abundance of smelt larvae, (D) mean length (mm) of smelt larvae, (E) abundance of *N. americana*, (F) abundance of *G. tigrinus*. L.T. = low tide, H.T. = high tide. Dark horizontal bars indicate night hours and open horizontal bars, dawn and dusk.

probably underestimated, as large numbers of juvenile organisms, of which only a part are retained by the 0.5-mm plankton net, were observed in our samples. In addition, the presence of egg-bearing *N. americana* and *M. stenolepis* indicate continued reproduction at the end of July. In the colder waters of Passamaquoddy Bay, the three principal invertebrate species all reproduce in spring or summer: *N. americana* from July to October (Pezzack and Corey 1979), *M. stenolepis* in May and June (Amaratunga and Corey 1975), and *G. tigrinus* from April to October (Bousfield 1973). We may thus consider the maximum turbidity zone an important site of secondary production, particularly as many of these organisms are characterized by high turn-over rates (e.g., P/B of 3.66 for *N. americana* and 3.82 for *C. septemspinosus* in Long Island Sound (Richards and Riley 1976)). As these species are known to feed on detritus (*N. americana, M. stenolepis, G. tigrinus*) as well as microplanktonic (*N. americana*) and benthic (*C. septemspinosus*) prey items and are themselves preyed upon by larval smelt (Dauvin and Dodson, in preparation), the maximum turbidity zone plays a major role in the trophic dynamics of the middle estuary.

Within the MTZ, the distribution of *N. americana* appears to be associated with the position of the null zone. Although average maximum densities were observed at station 2 (Table 2), the analysis of the temporal structure of the communities revealed that maximum densities of *N. americana* occurred at station 3 at the end of flood, whereas at station 2, flood tides were generally characterized by lower densities of this species. These results suggest that the center of distribution of *N. americana* was located between the two stations, an area that approximately coincides with the estimated position of the null zone. Thus, the distribution of *N. americana* in the St. Lawrence estuary is similar to that of *N. mercedis* in the San Francisco Bay estuary where a diel vertical migration pattern is hypothesized to interact with two-layered estuarine flow and the turbid entrapment zone to prevent the population from being swept downstream (Orsi 1986). Although a similar mechanism may be responsible for the retention of *N. americana* in the St. Lawrence MTZ, our 48-h sampling series does not permit a meaningful analysis of diel vertical migrations.

Smelt larvae are distributed further upstream within the MTZ than *N. americana* and their distribution appears to be size-dependent. Average maximum densities of larvae were observed at station 3 (Table 2). The high densities of larvae observed during ebb tides indicates that they are present upstream of station 3. This is consistent with the calculation of net upstream larval flux at this station. The upstream extent of larval smelt distribution is unknown. The observation at station 2 that large and intermediate smelt larvae are associated with ebb tides whereas small smelt larvae are characteristic of flood tides indicates that the distribution of larger smelt larvae is centered upstream of station 2, whereas that of smaller larvae is downstream. This is consistent with the observation that principally small larvae are observed downstream at station 1 and intermediate and large smelt larvae are proportionately more abundant at station 3 (Table 2). However, the observation at station 3 that mean length tended to decrease during ebb tides and that the intermediate length class of larvae was characteristic of the water masses sampled during ebb tides suggests that the intermediate size class was located upstream of station 3, with the center of distribution of large smelt larvae occurring between stations 2 and 3 in the vicinity of the null zone.

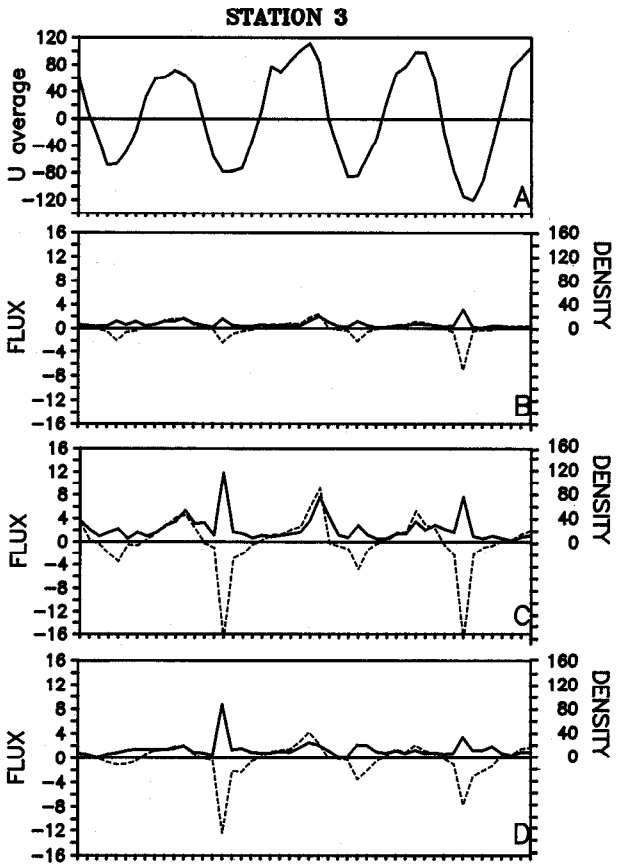

Fig. 10. Density and flux of smelt larvae at station 3. Panel A. Average depth-integrated longitudinal current velocity (cm s^{-1}) measured during the study period (positive values, downstream; negative values, upstream). The density (n 100 m^{-3}) and depth-integrated flux (n m^{-1} s^{-1}) of smelt larvae <25 mm, 25–30 mm, and >30 mm are presented in panels B, C, and D, respectively. The solid line illustrates larval density and the dotted line illustrates larval flux (positive values, downstream; negative values, upstream).

In summarizing the effects of circulation on lar-

val densities and net flux, one finds the study area between stations 2 and 3 to be a region of retention or longer residence time. Overall, larger larvae are distributed further upstream than smaller larvae. We presume that the retreat of the null zone over the study period caused the locus of the three size groups to move upstream. However, due to the depth contours of the estuary and the Coriolis force, flooding waters preferentially follow the north channel whereas ebbing waters preferentially follow the south channel (Ouellet and Cerceau 1976; Kranck 1979). As a result, the null zone is skewed across the estuary (further upstream on the north side) and adds complexity to the analysis of data taken at stations along the estuarine major axis. As smaller larvae are most probably distributed further upstream in the north channel, the downstream advection at station 3 of small larvae during ebb tide may be the result of cross-channel transport of small larvae from the north to the south side of the estuary on the ebbing tide. This argument is supported by the observation of strong cross-channel flow (SE) at the deeper moored current meter (station C) at the start of the ebb flow for each tide cycle. As the average depth-integrated cross-channel flux of larvae at stations 2 and 3 was to the north shore, we propose that the general cyclonic circulation of the area probably contributes to retaining larvae in the upper estuary. Cyclonic circulation has also been proposed to play a role in the maintenance of larval herring (*Clupea harengus*) in the downstream section of the middle estuary. Based on observations at an anchor station located 60 km downstream of Ile aux Coudres in the deep north channel, Fortier and Leggett (1983) proposed that the large-scale cyclonic circulation prevailing at depth is responsible for the retention of early postlarval herring in the middle estuary. Larval herring, however, have not been observed to penetrate upstream into the maximum turbidity zone (Laprise, unpublished data).

Although the spatial distribution of *N. americana*, *Gammarus* sp. (principally *G. tigrinus*), larval smelt, *Mysis stenolepis*, and *Crangon septemspinosus* in the middle estuary was associated with the maximum turbidity zone, temporal fluctuations in the abundance of these species were not related to fluctuations in turbidity. At station 2, discriminant analysis revealed that the three sample groups were separated mainly on the basis of salinity and temperature. Partial correlation coefficients computed from the pooled covariance matrix revealed that turbidity was not correlated with either salinity ($r = -0.06$, $p = 0.458$) or temperature. Similarly, salinity and temperature were mainly responsible for the separation of the three sample groups of station 3. Neither salinity ($r = 0.03$, $p = 0.743$) nor temperature ($r = -0.04$, $p = 0.663$) was correlated with turbidity. However, instantaneous values of turbidity vary as a function of velocity because of local resuspension as well as advection. Thus individual sample comparisons might not reveal a statistical relationship between macroplankton and turbidity.

In conclusion, smelt in the middle estuary of the St. Lawrence are associated with a highly productive planktonic community that provides an abundant source of food beginning with the earliest life history stages (Dauvin and Dodson, in preparation). The relationship between turbidity and larval density at a specific time is weak (because of sediment resuspension but not larval), but the mechanism responsible for producing higher residence times for both sediment and larvae on a longer term basis is the same. The daily movement and skewed nature of the null zone does not allow selection of any specific location for larval concentration but indicates a geographic zone over which the population oscillates for some time and remains independent of the mean downstream velocities over the water column.

Acknowledgments

We thank P. Picard, H. Dompierre, M. Dubé, J. Basmajdian, N. Martel, B. Massicotte and D. Robert for their assistance in the field and J.-J. Frenette and R. Laprise for advice and assistance in statistical analysis. This project was supported by grants from FCAR to J. J. Dodson, R. G. Ingram and GIROQ (Groupe Interuniversitaire de Recherche Océanographiques du Québec). The participation of J.-C. Dauvin was made possible by a leave of absence granted by the Centre National de la Recherche Scientifique (France) and scholarships provided by NATO and Le Ministère des Relations Internationales du Québec.

Literature Cited

Able, K. W. 1978. Ichthyoplankton of the St. Lawrence estuary: Composition, distribution, and abundance. *J. Fish. Res. Board Can.* 35:1518–1531.

Amaratunga, T., and S. Corey. 1975. Life history of *Mysis stenolepis* (Smith) (Crustacea, Mysidacea). *Can. J. Zool.* 53:942–952.

Barclay, W. R., and A. W. Knight. 1981. The nutritional significance of the distribution of suspended particulate material in the upper San Francisco Bay estuary, p. 55–70. *In* R. D. Cross, and D. L. Williams (eds.), Proceedings of the National Symposium on Freshwater Inflow to Estuaries, Vol. 1. U.S. Department of the Interior, Washington. FWS/OBS-81/04.

Bousfield, E. L. 1973. Shallow-water gammaridean Amphipoda of New England. Cornell Univ. Press, Ithaca. 312 p.

Bousfield, E. L., G. Filteau, M. O'Neill, and P. Gentes. 1975. Population dynamics of zooplankton in the middle St. Lawrence Estuary, p. 325–351. *In* L. E. Cronin (ed.), Estuarine Research, Vol. 1. Academic Press, New York.

Cardinal, A., and L. Berard-Therriault. 1976. Le phytoplancton de l'estuaire moyen du Saint-Laurent en amont de l'Ile-aux-Coudres (Québec). *Int. Revue Ges. Hydrobiol.* 61:639–648.

COURTOIS, R., M. SIMONEAU, AND J. J. DODSON. 1982. Interactions multispecifiques: Répartition spatio-temporelle des larves de capelan (*Mallotus villosus*), d'éperlan (*Osmerus mordax*) et de hareng de l'Atlantique (*Clupea harengus harengus*) au sein de la communauté planctonique de l'estuaire moyen du Saint-Laurent. *Can. J. Fish. Aquat. Sci.* 39:1164–1174.

D'ANGLEJAN, B. F. 1981. On the advection of turbidity in the Saint-Lawrence Middle Estuary. *Estuaries* 4:2–15.

D'ANGLEJAN, B. F., AND R. G. INGRAM. 1984. Near bottom variations of turbidity in the Saint-Lawrence Estuary. *Estuarine Coastal Shelf Sci.* 19:655–672.

D'ANGLEJAN, B. F., AND E. C. SMITH. 1973. Distribution, transport, and composition of suspended matter in the St. Lawrence estuary. *Can. J. Earth Sci.* 10:1380–1396.

FORTIER, L., AND W. C. LEGGETT. 1983. Vertical migration and transport of larval fish in a partially mixed estuary. *Can. J. Fish. Aquat. Sci.* 40:1543–1555.

GOBEIL, C., B. SUNDBY, AND N. SILVERBERG. 1981. Factors influencing particulate matter geochemistry in the St. Lawrence estuary turbidity maximum. *Mar. Chem.* 10:123–140.

HANSEN, D. V., AND M. RATTRAY. 1966. New dimensions in estuarine classification. *Limnol. Oceanogr.* 11:319–326.

KRANCK, K. 1979. Dynamics and distribution of suspended particulate matter in the Saint-Lawrence Estuary. *Le Natur. Can.* 106:163–173.

LANCE, G. N., AND W. T. WILLIAMS. 1967. A general theory of classificatory sorting strategies. I. Hierarchical systems. *Computer J.* 9:373–380.

LEGENDRE, L., AND P. LEGENDRE. 1984. Ecologie numérique, Tome 2. La structure des données écologiques. Masson, Paris et les Presses de l'Université du Québec, 2e édition, VIII + 335 p.

LEGGETT, W. C. 1985. The role of migrations in the life history evolution of fish, p. 277–295. *In* M. A. Rankin (ed.), Migration: Mechanisms and Adaptive Significance. *Contr. Mar. Sci.* 27:353–366.

LEGGETT, W. C. 1984. Fish migrations in coastal and estuarine environments: A call for new approaches to the study of an old problem, p. 159–178. *In* J. D. McCleave, G. P. Arnold, J. J. Dodson, and W. H. Neill (eds.), Mechanisms of Migration in Fishes. Plenum Press, New York.

LUCOTTE, M., AND B. D'ANGLEJAN. 1986. Seasonal control of the Saint-Lawrence maximum turbidity zone by tidal flat sedimentation. *Estuaries* 9:84–94.

MAUCHLINE, J. 1980. The biology of mysids. *Adv. Mar. Biol.* 18:1–97.

MILLER, J. M., L. B. CROWDER, AND M. L. MOSER. 1985. Migration and utilization of estuarine nurseries by juvenile fishes: An evolutionary perspective. *In* M. A. Rankin (ed.), Migration: Mechanisms and Adaptive Significance. *Contr. Mar. Sci.* 27:338–352.

NIXON, S. W. 1981. Freshwater inputs and estuarine productivity, p. 31–57. *In* R. D. Cross, and D. L. Williams (eds.), Proceedings of the National Symposium on Freshwater Inflow to Estuaries, Vol. 1. U.S. Department of the Interior, Washington. FWS/OBS-81/04.

ORSI, J. J. 1986. Interaction between diel vertical migration of a mysidacean shrimp and two-layered estuarine flow. *Hydrobiologia* 137:79–87.

OUELLET, P., AND J. J. DODSON. 1985. Dispersion and retention of anadromous rainbow smelt (*Osmerus mordax*) larvae in the middle estuary of the St. Lawrence River. *Can. J. Fish. Aquat. Sci.* 42:322–341.

OUELLET, Y., AND J. CERCEAU. 1976. Mélange des eaux douce et salées du Saint-Laurent: Circulation et salinité. *Les Cahiers de Centreau* 1, 57 p.

PETERSON, D. H., J. J. CONOMOS, W. W. BROENKOW, AND P. C. DOHERTY. 1975. Location of the non-tidal current null zone in northern San Francisco Bay. *Estuarine Coastal Mar. Sci.* 3: 1–11.

PEZZACK, D. S., AND S. COREY. 1979. The life history and distribution of *Neomysis americana* (Smith) (Crustacea, Mysidacea) in Passamaquoddy Bay. *Can. J. Zool.* 57:785–795.

POSTMA, H. 1967. Sediment transport and sedimentation in the estuarine environment, p. 158–179. *In* G. H. Lauff (ed.), Estuaries. American Association for the Advancement of Science, Publication 83. Washington, D.C.

RICHARDS, S. W., AND G. A. RILEY. 1967. The benthic epifauna of Long Island Sound. *Bull. Bingham Oceanogr. Collection* 19: 89–129.

SIEGFRIED, C. A., M. E. KOPACHE, AND A. W. KNIGHT. 1979. The distribution and abundance of *Neomysis mercedis* in relation to the entrapment zone in the western Sacramento-San Joaquin delta. *Trans. Am. Fish. Soc.* 108:262–268.

WIGLEY, R. L., AND B. R. BURNS. 1971. Distribution and biology of mysids (Crustacea, Mysidacea) from the Atlantic Coast of the United States in the NMFS Woods Hole collection. *Fish. Bull.* 72:835–842.

ZAGURSKY, G. AND R. J. FELLER. 1985. Macrophyte detritus in the winter diet of the estuarine mysid, *Neomysis americana*. *Estuaries* 8:355–362.